

Thesis Chapter: Calibration Source & GPS

Tom Laclavère

17 février 2025

Table des matières

1	Introduction	2
2	Calibration for QUBIC	2
2.1	Self-Calibration	2
2.2	Calibration Source's characteristics	3
2.3	Calibration procedure	4
2.3.1	Calibration Time (title??)	4
2.3.2	Calibration Tower	5
2.3.3	Equivalent 2 horns open procedure (title??)	6
3	GPS	6
3.1	Characteristics	8
3.2	GPS Data	9
3.2.1	Binary to numerical conversion (necessary?)	9
3.2.2	Backward-engineering	9
3.2.2.1	Relative Position Vector	9
3.2.2.2	GNSS Angles	10
3.2.2.3	IMU Angles	11
3.3	Antennas' Position	11
3.4	Noise Analysis	12
4	Calibration Source position and orientation	13
4.1	System limitations and Hypothesis	13
4.1.1	Communication with satellites	13
4.1.2	System rigidity	13
4.1.3	Rotation around antennas vector	13
4.2	Initial Configuration	14
4.3	Calibration Source Position	15
4.4	Calibration Source Orientation	15
4.5	Results	15
5	Data on Site	16

1 Introduction

Minimizing the instrumental effects is one of the most important goals, with the reduction of foreground contamination, of experiments targeting B-mode patterns in the CMB. An accurate calibration of the instrument is needed to achieve a high sensitivity. In addition to classical calibration, an innovative method based on radio-interferometry[5], called self-calibration, was thought for QUBIC. This method relies on comparing the different baselines of an interferometer to characterize its systematic effects. In this context, an accurate knowledge of the calibration source position and orientation is needed. A GPS will be used for this purpose.

In this chapter, we aim to explain the calibration method for the QUBIC instrument, and in particular, the GPS associated with the Calibration source, its characteristics, and its use within the calibration procedure, including a study of the noise of this system. My contributions are related to the study of GPS. I ran tests to understand its functioning and the meaning of the output data. I also ran an analysis on the noise of this system, which will be used to choose the best way to install it on the observation site. This work will be presented in section 3. Then, I wrote a software adapted to our specific use that I will detail in section 4. Finally, the installation on the observation site and the first data from the system are described in section 5.

2 Calibration for QUBIC

We will describe the calibration method for a Bolometric Interferometer as QUBIC. This method, called "self-calibration", is based on the observation and the comparison of a known calibration source through different interferometer baselines, using a simple formalism to understand its principle. Then, the calibration source that will be used to self-calibrate the QUBIC Instrument and the associated specific calibration procedure will be discussed.

2.1 Self-Calibration

The self-calibration method for QUBIC was developed by Marie-Anne Bigot-Sazy during her PhD, you can find the details in her thesis[2] and her published paper on the topic[4].

Bolometric Interferometry differs from other CMB instruments by its interferometric aspect, leading to the possibility of doing self-calibration. The idea consists of comparing the image of a known source by observing different baselines to estimate systematic effects. The simplest case is to compare redundant baselines, for example, two pairs of horns separated by the same distance, as shown in Figure 1. In this case, we should observe the same interference pattern for both baselines for an ideal instrument. With systematic effects, we will observe differences between the two patterns, due to systematic effects (size of

horns, position of horns, mirror misalignment, ...). However, we are not limited to redundant baselines and can use any baseline of the instrument in this method. By comparing all the different baselines of the interferometer, we will then have a lot of information on these effects, allowing us to characterize and reduce them.

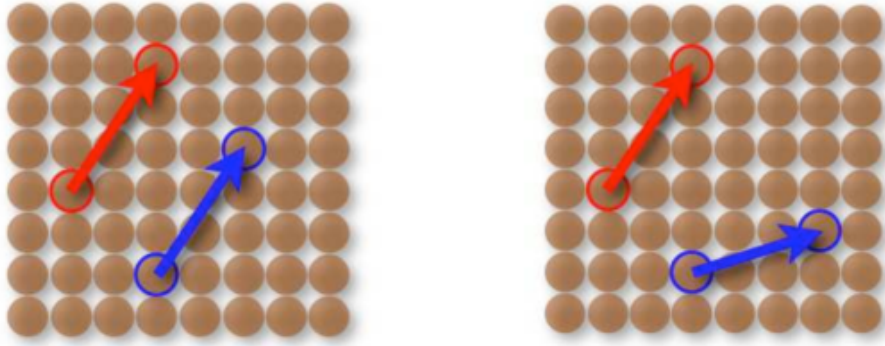


FIGURE 1 – Illustration showing two redundant baselines on the left, and two non-redundant baselines on the right. Taken from [3]

This method is only possible if we have more baselines to compare than parameters describing the instrumental systematics. For the QUBIC Full Instrument, the horns array should contain 400 horns[6], meaning $n(n - 1)/2 = 79800$ baselines, which will be largely sufficient for this purpose [ref??](#).

[Do I need to develop more on the method ?](#)

2.2 Calibration Source's characteristics

[How far do I need to develop in this section ?](#)

All the technical details concerning the calibration source and its utilization are described in the QUBIC Laboratory Characterization paper[7]. We propose here to summarize the information from this article.

The calibration source system has been purchased from **Virginia Diodes Incorporated (VDI) electronics**¹. It is composed of two parts : the source itself and the electronics to control it. The frequency range of the source is between 130 and 170 GHz ([Only for the TD I guess](#)), as for the QUBIC Instrument, with a tuning resolution of 144 Hz.

The calibration source and its electronics will be placed in a calibration box to protect them from weather conditions. This box acts as a Faraday cage to avoid electromagnetic disturbances. Insulating foam is also glued to the walls of the box to limit acoustic perturbations. You can find pictures of the inside and outside of the calibration box in Figure 3.

1. <https://vadiodes.com>

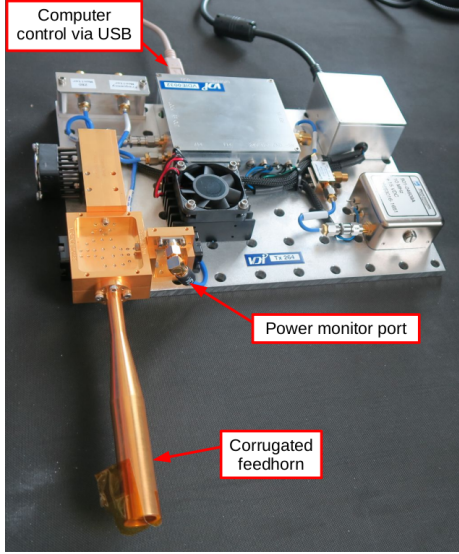


FIGURE 2 – Picture of the calibration source system, including its electronics and the waveguide horn. Taken from [7]

2.3 Calibration procedure

As discussed previously, the calibration procedure for a Bolometric Interferometer such as QUBIC is different from the one for an imager (Do I need to describe more precisely the difference between the two ? I think there is a section discussing that in Marie-Anne's thesis.). QUBIC has specific constraints regarding the calibration process, that we will present in this section. An important comment is that self-calibration can take place in parallel with the observation process, as it allows us to estimate the systematic effects and take them into account in the data analysis algorithms afterward. (Put this remark in the following section ??)

2.3.1 Calibration Time (title ??)

An important specificity of the QUBIC Instrument is that its target sky patch is not always visible (I would like to have more information on this information. Do we have a reference to compute the fraction of time when the patch will be visible ?). This patch is centered on the ($RA = 0^\circ$, $DEC = 57^\circ$) position, known for its low dust emission, and representing 1.5% of the entire sky. Thus, we can take advantage of this not-observing time to perform self-calibration, as it will increase sensitivity. As said before, it's not mandatory to self-calibrate before observation, we can run both in parallel and use the systematics characterization from the self-calibration to improve the data analysis process during the whole observation program.

It has been shown in [4] that spending 1 s to calibrate per baseline can improve

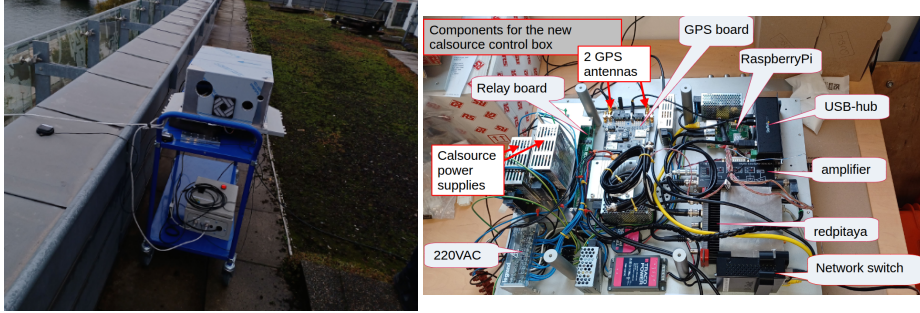


FIGURE 3 – (left) Photo of the calibration box, on top of the chariot. ([Add notes to distinguish reference antenna from the others on the picture](#)). (right) Photo of the inside of the calibration box. The GPS PCB is included within the box. The integration was made by Claude Boutonnet at APC.

the leakage from E to B modes by one order of magnitude, while it can improve it by two orders of magnitude when spending 100 s per baseline. This second case corresponds to spending 100 seconds for each of the 79800 baselines, meaning 91 days of observation (approximately 25% of the observation time in one year). This work was done ten years ago, a more up-to-date analysis is needed to confirm these predictions. ([Do we know the time fraction when the patch will be visible for three years ? To be sure that the previous sentence makes sense... Maybe we can use the framework from Elenia to compute that..](#))

2.3.2 Calibration Tower

The QUBIC Collaboration has chosen to use a tower to hold the Calibration Source. This choice is motivated by the need for self-calibration of long-time observation of the calibration source (allowed by the time when the sky patch will not be in the instrumental field of view, see previous sub-section).

This tower has to respect different constraints for the observation. It has to be high enough to be in the field of view of the instrument and to avoid the ground emission and far enough to consider the source as a point source. Also, the tower should not perturb the observation of the target sky patch.

As shown in [7], the calibration source can be considered at an infinite distance even at 11.4 m from the instrument, as the angular resolution of QUBIC is particularly low (even the moon is seen as a point source). The tower distance is then, not a strong constraint. To be visible from the instrument, the tower's height is about 54 m, while the distance to the QUBIC shelter is approximately 65 m. The calibration source will be placed close to the anti-rotation structure, visible Figure 4, around 50 m from the ground. Knowing that the QUBIC instrument is at ??? m from the ground ([Ask height of QUBIC from the ground](#)), the calibration will be seen at an elevation of about ??? °. Also, the calibration tower has been put at the North of the instrument, to avoid the situation where the tower can be in front of the target sky patch.

Finally, the last requirement for the tower is its movement. Because the tower is tall, and located in a place with strong wind, it is mandatory to prevent the displacement of the structure. Otherwise, the calibration source will not point directly at the instrument window, meaning a phase shift and a lower amplitude for the observed signal, which can lead to an issue for calibration. As said just above, the tower has an anti-rotation structure, where the calibration source will be placed. But, in the case where the tower can still move, a GPS was thought to track the deviated position and orientation of the source and then be able to compute the received power from the source to the instrument. This system will be detailed in the third part of this chapter, section 3.



FIGURE 4 – Photo of the calibration tower, with the heights of the tower and of the top and bottom of the anti-rotation structure ([find a better picture](#))

2.3.3 Equivalent 2 horns open procedure (title ??)

This section should discuss the fact that if we open only two horns, the bolometers will not be heated enough to be at the superconductivity transition (if they are configured to be at this transition when all the horns are open). Then, we need to find a way to have a procedure equivalent to opening two horns, when opening more than 2 horns to avoid this issue.

3 GPS

For calibration, it is mandatory to know exactly the signal coming from the source. We described the characteristics of this source in section 2.2. But, it is

not enough, as the calibration source will move with the calibration tower because of wind. This change in position and orientation can lead to a significant modification of the signal observed by the instrument. An analysis was run by Sabrina Marwede, PhD student from Maynooth University working on the optic simulations for QUBIC, to observe the effect of such deviation on the amplitude of the received signal. One example can be found in Figure 5.

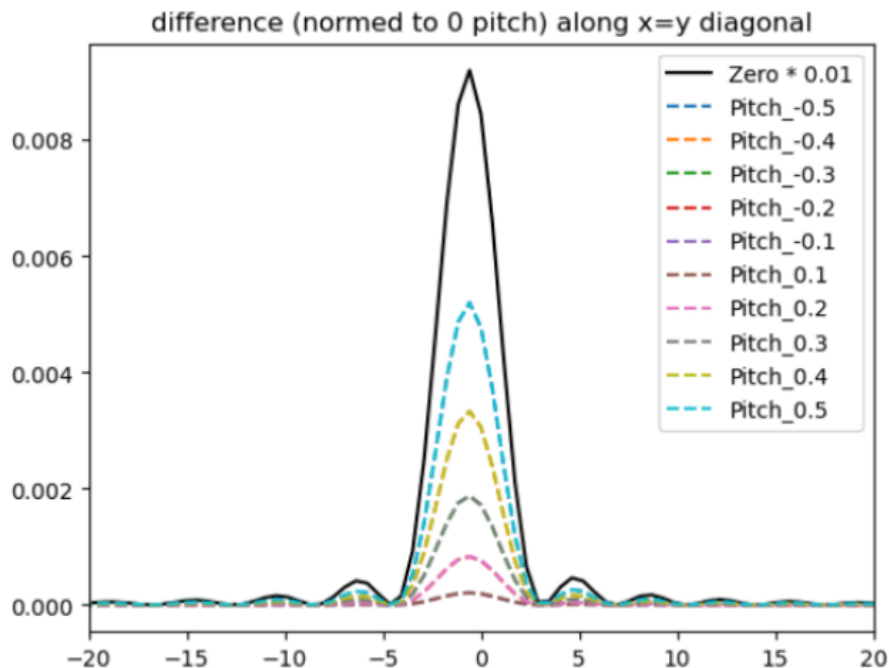


FIGURE 5 – Plot showing the decreasing of the amplitude of the signal observed by QUBIC with the deviation of the calibration source line of sight. Simulation made by Sabrina Marwede from Maynooth University. (IMPORTANT : need to discuss with Sabrina about this work + need to find a better plot (or to redo it))

It becomes important to track these displacements to avoid accuracy losses during the self-calibration process. A GPS (Global Positioning System) will be used for this purpose.

3.1 Characteristics

The GPS was purchased from **ArduSimple**² and its native software was designed by **EPS Works**³. This system is composed of three antennas and electronics to process the data. Pictures of the antennas and the GPS card can be found in Figure 6. Within these antennas, one will be fixed with a known position, called "base antenna". The two others can move and the system will compute their relative position to the fixed one. We will call them "Antenna 1" and "Antenna 2". This kind of system is called Real Time Kinetic (RTK), and it is used for tracking or plane autopilot for example. Of course, the precision on the absolute position is limited by the precision on the base antenna position. The typical accuracy of this system is typically of the order of 1 cm (ref??). We will verify that during the noise analysis, section 3.4.

The position of the receivers is computed by communicating with geostationary satellites. The internal clock of both the receiver and the satellite being synchronous, the receiver will determine the time shift introduced by the travel of light across the atmosphere to compute the distance with the satellite. When you have at least 3 satellites, you can use this method to compute the position of the antenna on Earth (Add a schema to describe that, maybe from https://docs.centipede.fr/docs/centipede/2_RTK.html). Different phenomena can produce errors during this computation, for example : if the signal is reflected, if the two clocks are not synchronized, if the slowdown of the signal within the ionosphere or troposphere is wrongly estimated, etc. (More detailed can be found on : https://en.wikipedia.org/wiki/Real-time_kinematic_positioning)

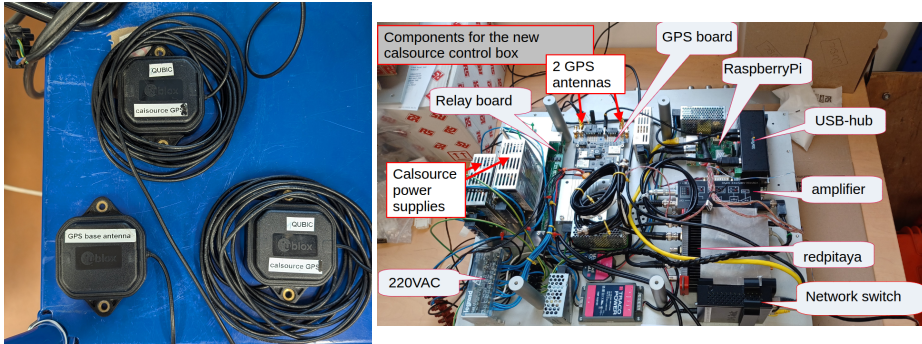


FIGURE 6 – (left) Picture of the three antennas (Add notes to distinguish reference antenna from the others on the picture). (right) Picture of the inside of the calibration box. The GPS PCB is included within the box. (Need to take a picture of only the GPS parts)

2. <https://fr.ardusimple.com/>
 3. <https://www.eps-works.com/>

3.2 GPS Data

After describing the GPS, we will focus on understanding the data given by it. In particular, a backward-engineering work was done to correctly interpret some of them.

3.2.1 Binary to numerical conversion (necessary?)

The output data are in binary. We need a program to convert them into proper numerical values. Do I need to describe that?

3.2.2 Backward-engineering

According to the provider, and after converting the raw GPS date from binary, we have access to different data on the system, resumed in a table in Figure 7. In this chapter, we will focus on the data from 1 to 8. Unfortunately, we didn't how each of these data is defined. We set some simple tests to understand them, illustrated in the following sub-section.

Description	Generic status message				
Direction	simpleRTK2B-SBC -> USB				
Type	Output				
Comment	Attitude, Position (relative to fixed base) and Status of the moving base setup.				
Information	Number of fields: 11				
Structure	\$GPAPS,time,RPN,RPD,RPD,pitch,roll,yaw,pitchIMU,rollIMU,temp*cs\r\n				
Example	\$GPAPS,235959.999,101251,701251,503298,2542,359123,985,2685,254*6C\r\n				
Payload contents					
Field	Name	Format	Unit	Example	Description
0	GPAPS	string	-	\$GPAPS	APS message ID
1	time	hhmmss.sss	-	235959.999	UTC time
2	rpN	numeric	0.1mm	101251	North component of relative position vector
3	rpE	numeric	0.1mm	701251	East component of relative position vector
4	rpD	numeric	0.1mm	503298	Down component of relative position vector
5	roll	numeric	0.001deg	2542	GNSS calculated roll angle
6	yaw	numeric	0.001deg	359123	GNSS calculated yaw angle
7	pitchIMU	numeric	0.001deg	985	IMU calculated pitch angle
8	rollIMU	numeric	0.001deg	2685	IMU calculated roll angle
9	temp	numeric	0.1degC	254	Internal temperature
10	*cs	hexadecimal	-	*6C	Checksum
11	CRLF	character	-	\r\n	Carriage return and line feed

FIGURE 7 – Table resuming the data provided by the GPS.

3.2.2.1 Relative Position Vector

The first data that we can look at is the relative position vector, called rpN, rpE, and rpD. These three quantities correspond to the relative position (to the base antenna) on respectively the North, Est, and Down axes. To understand which position it gives, we set a very simple experiment. The base antenna

stays fixed during all the tests. Then, we move one of the two antennas at different positions, and we do the same for the other one. An example of two configurations during these tests is visible in Figure 8a. After that, we can look at the data, and see when rpN, rpE, and rpD change, when we move the antenna 1 or the antenna 2. During this experiment, we moved antenna 1 between ??? and ???, and we moved antenna 2 between ??? and ????. According to the data shown in figure 8b, we can see that rpN, rpE, and rpD evolve only when new move the antenna 2. Then, we can conclude that these data correspond to the relative position of the antenna 2 in (North, East, Down) coordinates.

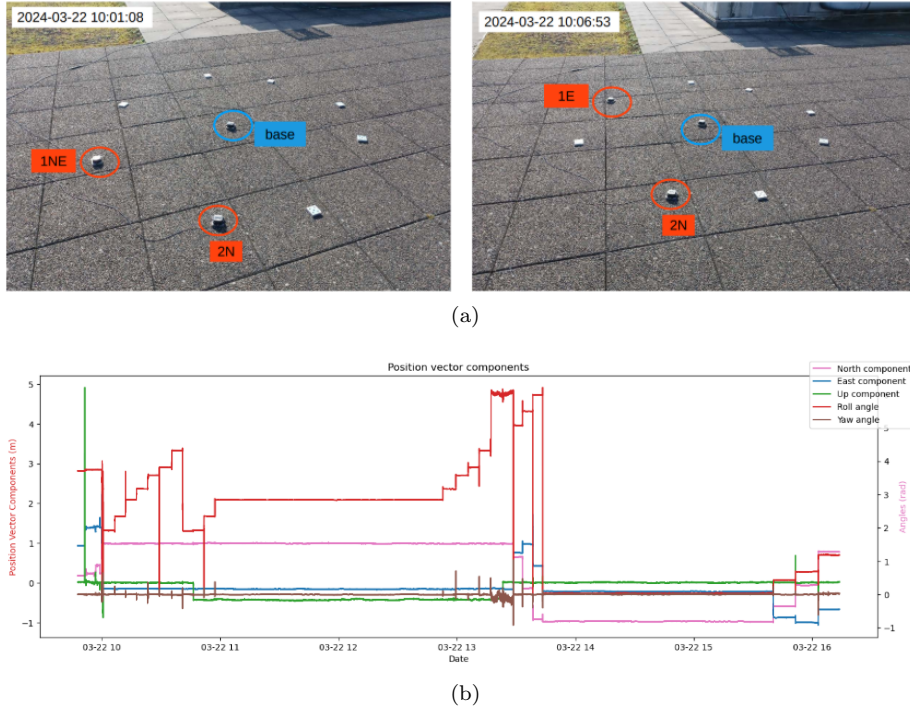


FIGURE 8 – (top) Example of two configurations during the experiment. (Describe a bit more the experiment + find a photo with better quality) (bottom) Plot of the different GPS data during the experiment. We can see that when we moved antenna 1 (between ??? and ???), the data didn't, while it was the case when we moved antenna 2 (between ??? and ???). (Need to redo this plot for this chapter)

3.2.2.2 GNSS Angles

The system does not provide the position of the second antenna directly, but the value of a roll and yaw angles. GNSS stands for Global Navigation Satellite System. It is a more general name to talk about using satellites to compute

position on Earth, GPS corresponding in fact to the specific satellite system developed by the USA.

We are used to the names "roll" and "yaw" to talk about two of the three rotation axes of an aircraft. They are not defined in the same way in our case. To understand their definitions, we can use the data from the experiment described in the previous subsection. In these data, we can see that the roll angle value evolved by step, with the different positions of the two antennas. Thus, roll angle has to be defined regarding the position of the two antennas. We found that it is defined as the angle between the North axis and the vector formed by the two antennas (from antenna 2 to antenna 1). We ran a more specific test to confirm this hypothesis by aligning the "antennas vector" at a known angle with the North axis using a compass and observing that we found the same value in the GPS data.

For the yaw angle, as its value did not change during all the previous tests, we made the hypothesis that it is defined with the vertical plane. Then, we tried to put the antennas at different heights for each other, and then compute the angle between the antennas vector and the ground. This angle corresponded to the yaw angle in the GPS data.

Add on another plot of the data here ? Pb : I don't think we kept data when we tried to understand the yaw angle.. Maybe I can redo that when I will test the IMU angles.

3.2.2.3 IMU Angles

IMU stands for Inertial Measurement Unit. It is a device that uses accelerometers and gyroscopes to measure the orientation of the system for navigation.
(I need to perform some tests before writing about it..)

3.3 Antennas' Position

Now that we understand the output data of the GPS, we can discuss how to use them to know the position and orientation of the calibration source in real-time. The first step for this purpose is to be able to compute the position of the two antennas. To summarize what was explained in the previous section, we have drawn a frame where the different data are illustrated, to represent what they correspond to, in Figure 9.

rpN , rpE , and rpD are the cartesian coordinates of antenna 2 in the (North, East, Down) frame, centered on the base antenna when roll and yaw are the angles between the antennas vector and respectively the North axis and the horizontal plane. This means that roll and yaw correspond to azimuth and elevation angles of antenna 1 in the spherical frame centered on antenna 2. Then, it is trivial to compute the position of antenna 2 : it is just three translations of rpN , rpE , and rpD from the (known) position of the base antenna. But, we miss one information to deduce the position of antenna 1 : the distance between the antennas. As the two have to stay fixed in our system (fixed with respect to the calibration source), we will need to measure the distance between the

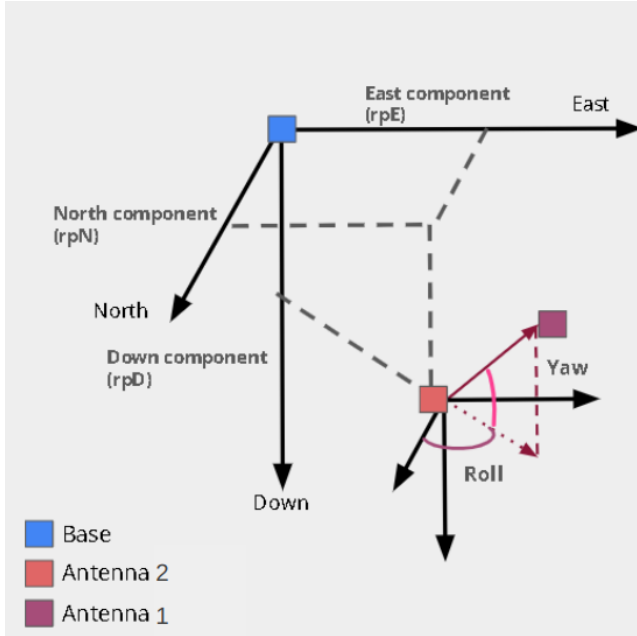


FIGURE 9 – Drawing of the different GPS output data. rpN, rpE, and rpD correspond to the relative position of antenna 1 in the (North, East, Down) cartesian coordinate system. Roll and Yaw correspond to azimuth and elevation angles between the two antennas. This picture was made by Eda Atav, a bachelor's student who worked with me on this topic during her internship.

two when the GPS will be installed on the calibration tower. Once this distance is known, we can compute easily the relative coordinate of antenna 1 with the base antenna using :

$$\begin{aligned}
 rpN_1 &= rpN_2 + d_{antennas} \cos(\text{roll}) \sin(\pi/2 - \text{yaw}), \\
 rpE_1 &= rpE_2 + d_{antennas} \sin(\text{roll}) \sin(\pi/2 - \text{yaw}), \\
 rpD_1 &= rpD_2 + d_{antennas} \cos(\pi/2 - \text{yaw}).
 \end{aligned} \tag{1}$$

3.4 Noise Analysis

At this point, we understand the output data of the GPS and we know how to compute the position of the two antennas. Before discussing how to use this information to compute the position and orientation of the calibration source, it is important to understand the noise properties of our system, in order to estimate its accuracy. We saw empirically that the noise amplitude increases when the antennas are close to each other. The idea is to understand how it evolves, and then to determine the best distance between them to minimize the noise level

of the system.

Work not done on this chapter. I need to fit the following noise model into the data I have :

$$P_{noise}(f) = A^2 \left(1 + \left(\frac{f_{knee}}{f}\right)^\alpha\right) \quad (2)$$

4 Calibration Source position and orientation

In this section, we will explain how the orientation and position of the calibration source are computed using the GPS described in section 3. In particular, we will need to discuss some limitations of this system, which lead to constraints on the installation of the system on-site.

4.1 System limitations and Hypothesis

As said before, the system suffers from intrinsic limitations. In order to resolve them, we will need to make some simplifying hypotheses and then constrain the system's installation.

4.1.1 Communication with satellites

The main issue we faced during our experiments was the signal loss from satellites. As described in section 3, we need to communicate with at least three satellites to compute positions. Also, the system needs some time to adjust with the satellites. Because of that, we needed to perform these tests on the roof of the APC laboratory's building, far from any obstacle. This should not be an issue on top of the calibration tower, but this problem is cited as it considerably slows down our tests.

4.1.2 System rigidity

To be able to compute the position and orientation of the calibration source using the antennas' position, we need to assume that the ensemble constituted of the calibration source, antenna 1 and antenna 2 is perfectly rigid. Firstly, and as explained in section 3.3, the distance between the two antennas needs to be fixed and known to compute the position of antenna 2. Then, for the same argument, the distance between antennas and the calibration source needs to be fixed and known to compute its position and orientation.

4.1.3 Rotation around antennas vector

Because we are using only two antennas, it happens that we can't reconstruct the calibration source's position and orientation in 3 dimensions : we are blind to one of them. In our case, and even if the system is rigid, we will always be blind to rotation around the antennas vector. This situation is illustrated in

Figure 10. As we are blind to rotation around this axis, and knowing the position of the antennas and the distances d_1 and d_2 with the source, it happens that the position of the calibration source is degenerated on the blue circle.

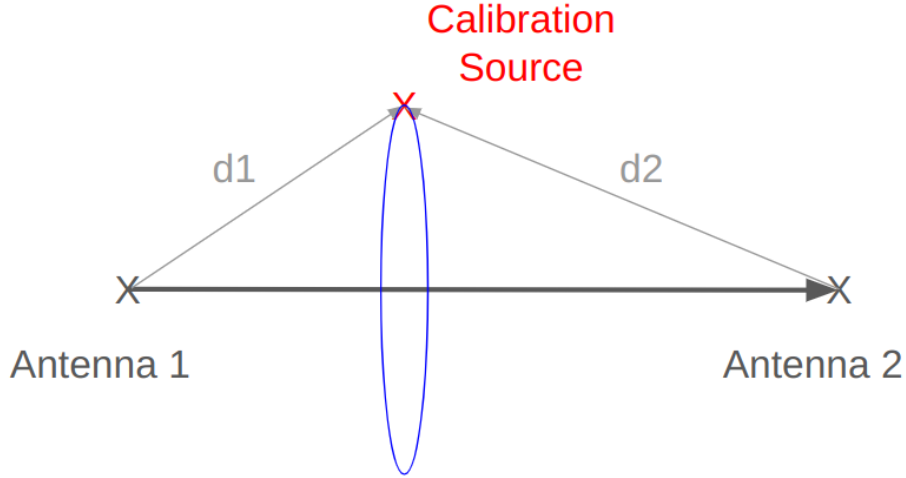


FIGURE 10 – Drawing to illustrate the fact that we are blind to rotation around the antennas' vector, the position of the calibration source can be anywhere on the blue circle.

To break this degeneracy, we need to make the hypothesis that there is no rotation around this axis. Of course, we can't impose that on a real system (but it will be reduced, thanks to the anti-rotation system installed on top of the calibration tower). To make this hypothesis reasonable, one can choose to place the source as close as possible to this axis. In this case, even if the system rotates around it, we will still be able to compute the position of the source as the rotation does not affect it.

Also, we have the same issue with the orientation of the calibration source : as we are blind to one rotation axis, the orientation is degenerated on a circle. To resolve this problem, we can set that the orientation of the source is aligned with the antennas vector. Then, and for the same reason as before, if the system rotates around this axis, we will still be able to compute the orientation of the source. This second hypothesis is only possible because the source is symmetrical, rotation around its orientation does not affect its signal.

4.2 Initial Configuration

The idea to compute the calibration source orientation and position at each time is to compare the movement of the system with respect to a known initial situation. As said in section 4.1, the source has to be placed on the antennas' axis, with its line of sight aligned with it. It is important to say that the software I

developed does not assume this specific situation, but because of the degeneracy discussed previously, it can be accurate outside this situation. When the GPS will be installed, the source will be placed in a way that it points exactly at the center of the QUBIC instrument. Then, during this initial condition, the source orientation and the antennas' axis will be aligned with the instrument's line of sight, and the distance between the source and the antenna will be measured. In this situation, it becomes simple to compute the orientation and the position of the source at any time.

4.3 Calibration Source Position

Under these hypotheses, it becomes simple to compute the position of the calibration source. Using the fact that we know the initial position of the antennas and that we can compute the current one, we can compute the system's translation. As the system is rigid, the source has undergone the same translation, allowing us to compute its position at each time.

4.4 Calibration Source Orientation

As said above, we will compute the orientation of the source by calculating the rotation between the initial and current antennas vector. As the system is rigid, the calibration will follow the same rotation from its initial orientation. Using general vectorial analysis, the rotation axis can be defined as the normal vector between the initial and rotated vector, given by :

$$\vec{n} = \frac{\vec{v}_1 \times \vec{v}_2}{\|\vec{v}_1 \times \vec{v}_2\|} \quad (3)$$

Then, the rotation angle α between two vectors is defined by the two following formulas :

$$\begin{aligned} \vec{v}_1 \cdot \vec{v}_2 &= |\vec{v}_1| \cdot |\vec{v}_2| \cdot \cos(\theta) \\ \vec{v}_1 \times \vec{v}_2 &= |\vec{v}_1| \cdot |\vec{v}_2| \cdot \sin(\theta) \end{aligned} \quad (4)$$

An important remark is that we want to avoid using \arcsin or \arccos , as they are defined respectively on $[-\pi/2, \pi/2]$ and $[0, \pi]$. We prefer to use \arctan , which is defined on $[-\pi, \pi]$, avoiding trigonometric issues. With this angle and the rotation axis of the rotation, it is easy to decompose it in rotation around the three axes of a cartesian frame using a specialized library like **Scipy Rotation**⁴, and then to retrieve the current orientation of the source.

4.5 Results

With these two steps, and under the discussed hypotheses, we can compute the position and orientation of the calibration source. An example of this is

4. <https://docs.scipy.org/doc/scipy/reference/generated/scipy.spatial.transform.Rotation.html>

given Figure 11. This plot is done with real data and confirmed by the software to build the previously described operations. We can also convert the position of the calibration source in azimuth and elevation from the QUBIC point of view. This representation can be more useful for the self-calibration process ([need to make a plot for this case](#)).

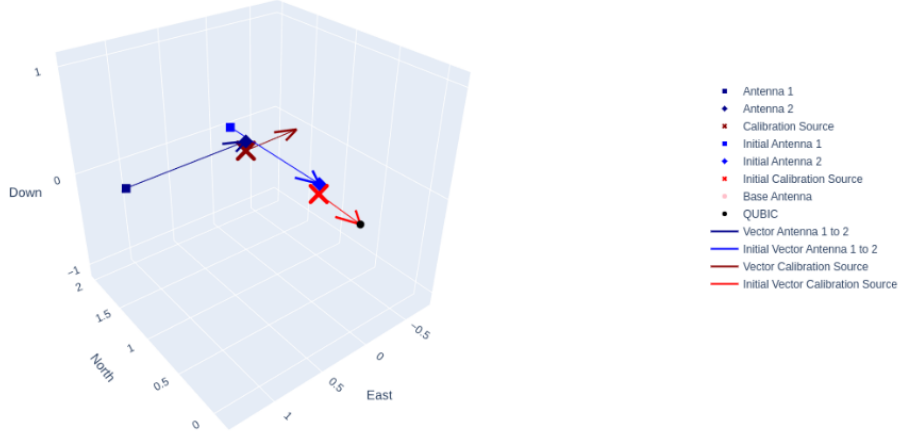


FIGURE 11 – Plot to illustrate how we reconstructed the position and orientation of the calibration source using the previous operations. The blue points give the initial position of the antennas while the red cross and arrow give the initial position and orientation of the source. We then moved the antennas and source, and were able to reconstruct the position and orientation of the source, as shown in dark blue and dark red.

5 Data on Site

[Not yet.](#)

Références

- [1] L. Mousset, "Exploring the primordial Universe, inflation and primordial gravitational waves with QUBIC, the Q and U Bolometric Interferometer for Cosmology", Phd Thesis, 2021.
- [2] M. A. Bigot-Sazy, "Mesure des anisotropies de polarisation du fond diffus cosmologique avec l'interferomètre bolométrique QUBIC", PhD Thesis, 2013.
- [3] R. Charlassier, "Mesure des anisotropies de polarisation du fond diffus cosmologique avec l'interféromètre bolométrique QUBIC," Paris 7, 2010, 1 vol. (244 p.) (Cit. on pp. 13, 34, 50).

- [4] M.-A. Bigot-Sazy et al., "Self-Calibration : an efficient method to control systematic effects in Bolometric Interferometry", A&A, vol. 550, p. A59, Feb 2013.
- [5] T. J. Pearson and A. C. S. Readhead, "Image formation by self-calibration in radio astronomy", Annual review of astronomy and astrophysics. Volume 22. Palo Alto, CA, Annual Reviews, Inc., 1984, p. 97-130.
- [6] J.-Ch. Hamilton et al., "QUBIC I : Overview and Science Program", 2021.
- [7] S.A. Torchinsky et al., "QUBIC III : Laboratory Characterization", 2022.